Density functional studies of catalytic alkane dehydrogenation by an iridium pincer complex with and without a hydrogen acceptor

Hua-Jun Fan, Michael B. Hall*

Department of Chemistry, Texas A&M University, TAMU 3255, College Station, TX 77843-3255, USA

Abstract

Density functional calculations have been applied to models of both transfer and acceptorless alkane dehydrogenation for the iridium(III) pincer complex, $(^RPCP)IrH_2$ ($^RPCP=\eta^3$-$C_6H_3(CH_2PR_2)_2$-1,3). The iridium pincer complex is the first efficient homogeneous catalyst that does not require photons or sacrificial hydrogen acceptors to drive the reaction, although with the latter the transfer reaction can accomplished under mild conditions. There are four essential steps for the catalytic cycle in both transfer and acceptorless reactions: oxidative addition of alkane, reductive elimination, β-hydrogen (β-H) transfer, and loss of olefin. The transfer reaction can utilize a hydrogen acceptor to produce a 14-electron intermediate, $(^RPCP)Ir(I)$, and the acceptorless reaction can produce an 18-electron intermediate, $(^RPCP)Ir(V)(H)_3(alkyl)$ species. Because the critical barriers are well-balanced in the Ir(V) catalytic cycle for acceptorless alkane dehydrogenation, no transition state (TS) is higher in energy than the products and no intermediate is lower in energy than the reactant. This balance could explain why pincer complexes are more efficient catalysts for alkane dehydrogenation than the corresponding Cp–Ir(III) complex. Entropy contributions, which play a larger role at high temperature, open new pathways for the acceptorless reaction. Free energies of activation suggest that the dynamics of the acceptorless reaction might be sampling the entire range of pathways and Ir oxidation states from Ir(I) to Ir(V).
© 2002 Elsevier Science B.V. All rights reserved.

Keywords: C–H activation; Alkane dehydrogenation; Iridium pincer complex; Density functional theory

1. Introduction

A challenging target for chemists is the direct and selective conversion of saturated hydrocarbons to more useful, functionalized organic compounds [1–7]. Because C–C and C–H bonds are strong (e.g. methane, C–H 105 kcal/mol), activation requires harsh or special reaction conditions. Direct alkane dehydrogenation is not only highly endothermic because of the C–H bond strength, but also has an extremely high barrier because it is a symmetry forbidden reaction. Fortunately, transition metals are able to catalyze these reactions by opening lower activation-energy pathways. However, the high endothermicity of the reaction requires driving the reaction photochemically [8–15] with UV irradiation or thermochemically [8–10,16–27] with either a sacrificial hydrogen acceptor or temperature. Most thermochemical dehydrogenation processes use a sacrificial hydrogen acceptor to make the process thermodynamically favorable [19–23]. This type of alkane dehydrogenation is called transfer dehydrogenation. Doing the reaction with heat, i.e. acceptorless dehydrogenation requires balancing the unfavorable equilibrium and catalyst

* Corresponding author. Tel.: +1-979-845-1843;
fax: +1-979-845-2971.
E-mail address: hall@mail.chem.tamu.edu (M.B. Hall).

decomposition. As a result, most research efforts have focused on finding catalysts that are both thermally stable and efficient.

Most homogenous catalysts surveyed are late transition metal complexes, such as Ru [28,29], Os [30–33], Rh [34–37], Ir [38–42], Pd [43–47], and Pt [48–53]. Among these catalysts, pincer complexes attracted considerable attention since their discovery by Moulton and Shaw [54]. The pincer ligand is η^3-$C_6H_3(CH_2PR_2)_2$-1,3 and is abbreviated as ^RPCP because the available chelating atoms of the pincer ligand are two P-arms and C from the arene ring. In this work, when R is unspecified, we are referring to the entire class of ligands. Other pincer-like ligands such as PCN [55] and NCN [56] are also under investigation. The meta-substituted C_6H_3 group in the pincer complex imposes a *mer* coordination geometry about the metal with a pair of *trans* phosphorus donors. Because these PCP-based catalysts appear to be stable for a period of time at elevated temperatures and have a high turnover rate [16–18], they make attractive catalysts for thermal dehydrogenation. Recently, Xu et al. [26] reported the first example of alkane dehydrogenation using $(^{t\text{-}Bu}PCP)IrH_2$ under reflux without the use of a sacrificial hydrogen acceptor. This type of thermochemical alkane dehydrogenation is referred to as acceptorless dehydrogenation. Later, they reported that the $(^{i\text{-}Pr}PCP)IrH_2$ complex shows higher turnover rate than $(^{t\text{-}Bu}PCP)IrH_2$ complex [27]. Recently, Haenel et al. reported a more effective catalyst in which the pincer ligand is replaced by anthracene-1,8-diphosphine (athraphos) [57].

These experimental studies have provided an opportunity for computational chemists to examine various mechanisms for these reactions. Hall and co-workers compared both acceptorless and transfer alkane dehydrogenation using $(^HPCP)IrH_2$ as a pincer Ir(III) model [58,59] and compared the reaction to a non-pincer Ir(III) complex. They discovered that the *mer* geometry stabilizes 16-electron Ir(III) complexes and weakens the metal–olefin interaction, which are both important factors for an efficient catalyst [57–64]. These effects are related to the fact that the *mer* geometry, as compared to a *fac* geometry, raises the energy difference between the singlet and triplet states of the transition metal fragment [58]. Thus, the constrained geometry is particularly important to the catalytic properties of the pincer complex.

Because the reactions occur at elevated temperature, Krogh-Jespersen et al. also examined the entropy contributions and the free energy of these reactions with the model $(^{Me}PCP)IrH_2$ [65]. Our most recent theoretical work on this "anthraphos" Ir complex raises the possibility of a new alternative pathway for these reactions [57]. All of these studies will be reviewed and the difference between transfer and acceptorless reactions (with or without a sacrificial olefin) will be described.

2. Theory

Hall and co-workers' studies [57–59] utilized density functional theory [66] with the B3LYP functional [67–70] to optimize the structures of intermediates and transition states (TSs). All of the TSs obtained in both studies were optimized by a quasi-Newton method [71], and verified by separate frequency calculations, which showed only one imaginary frequency [72]. The catalyst model used in both studies was $(^HPCP)IrH_2$, $(^HPCP=\eta^3$-$C_6H_3(CH_2PH_2)_2$-1,3). The basis set for Ir was the modified LANL2DZ [73,74] of Couty and Hall [75], whose outmost p-orbital was replaced by (41) split of an optimized 6p function. The basis set for P was the standard LANL2DZ basis set augmented by a d-type polarization function [73,76]. The effective core potential (ECP) was used for both Ir and P [73,74]. Slightly different basis sets were used for ^HPCP ligand. In the study without an H_2 acceptor [58], the Dunning–Huzinaga double-zeta basis set with polarization functions (D95**) was used for the metal-coordinated carbons and hydrogens [77], and the STO-3G basis set was used for the uncoordinated carbons and hydrogens in ^HPCP ligand. In the study with an H_2 acceptor [59], the 6-31G(d, p) basis sets were used for the metal-coordinated carbons and hydrogens [78], and the 3-21G basis set was used for the uncoordinated carbons and hydrogens in ^HPCP ligand [79]. The basis sets used by Haenel et al. [57] were the same as to those used in the transfer reaction [59]. Krogh-Jespersen et al. used LANL2DZ for Ir atom, the Dunning–Huzinaga double-zeta basis set for C [77] and McLean–Chandler basis set for P [80], triple-zeta with polarization function for dihydrogen and hydrides [81], and double-zeta for hydrogen atoms of alkyl or aryl of ^{Me}PCP [82].

In order to reduce size of the calculation for the acceptorless reaction, methane was used for the oxidative addition of alkane and reductive elimination of dihydrogen and ethane was only used for the β-hydrogen (β-H) transfer and olefin loss. These two energy profiles (one with methane in first two steps, and the other with ethane in the next two steps) are then linked together at intermediates after the reductive elimination. The energy profile with methane should be valid since previous work has shown that the relative energy changes are similar for these two alkanes [58]. These results reported here are the energies without zero-point and thermal corrections.
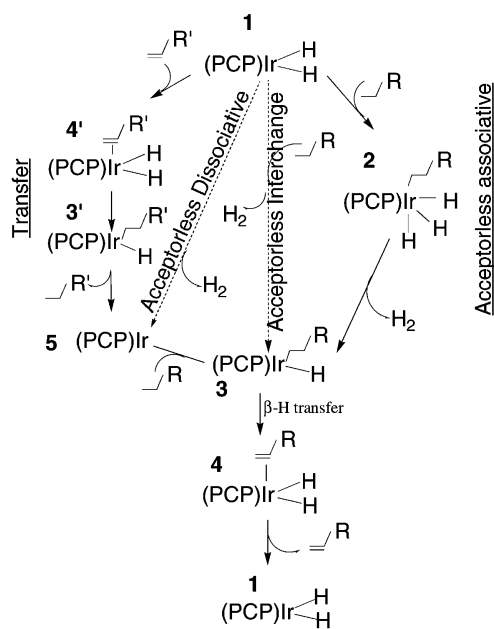
3. Results and discussion

Because of the presence of an H_2 acceptor, the transfer dehydrogenation proceeds at a much lower temperature than acceptorless dehydrogenation [26,27]. For example, the Ir(III) pincer complex, (PCP)Ir(H)$_2$, catalyzes the transfer dehydrogenation at temperatures as low as $100\,°C$ while the dehydrogenation reaction without an H_2 acceptor needs about $200\,°C$ [16]. Although these two reactions are clearly related, the large difference in the reaction conditions could lead to different reaction pathways involving different intermediates and TSs. Both experimental [10,23,24,83,84] and theoretical studies [57–64] have demonstrated that alkane dehydrogenation generally includes the following steps: (1) oxidative addition of the alkane, (2) reductive elimination of dihydride (acceptorless) or alkane (transfer), (3) β-H transfer between the alkyl ligand and the metal, (4) loss of coordinated olefin. Although these elementary steps are important for both reactions, their order in the mechanisms will differ [58,59]. Both reactions also involve a change by two in the formal oxidation state, but the actual oxidation state for the two reactions may differ. The transfer dehydrogenation reaction involves Ir(III) and Ir(I), while the lowest energy acceptorless dehydrogenation mechanism involves Ir(III) and Ir(V) species. The essential intermediates involved in the two reactions are summarized in the Scheme 1 and the reaction pathways are summarized in Scheme 2. Since the steps involved in $1 \rightarrow 3$ are identical for both reactions, we will discuss the steps involved in $1 \rightarrow 3$ in the transfer reaction and compare those results with the related steps
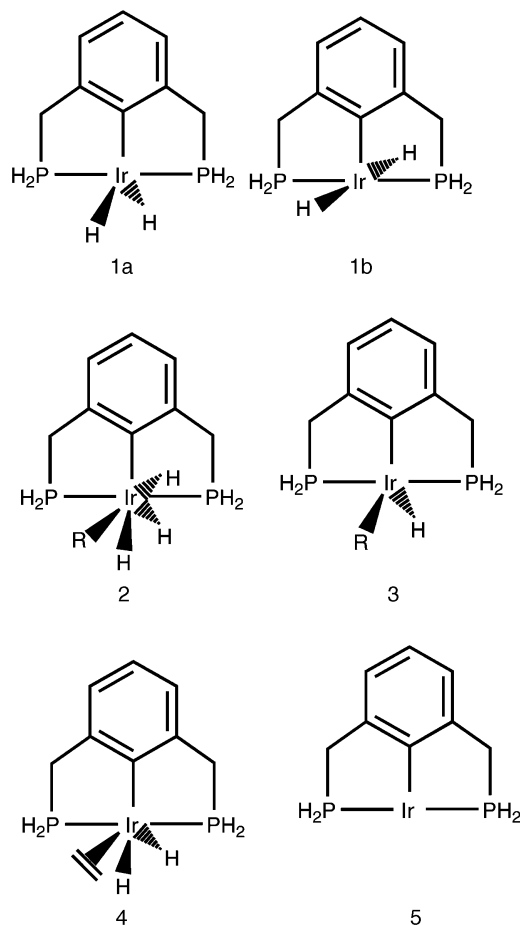
Scheme 1.

in acceptorless reaction before discussing $3 \rightarrow 4 \rightarrow 1$. The energy profile and the entropy contribution will be addressed after the description of these steps.

Niu and Hall found that the alkane dehydrogenation could start either with **1a** or with **1b**, see Scheme 1 [58]. The difference between these two structures lies mainly in the H–Ir–H angle (**1a** $= 62.7°$ and **1b** $= 176.6°$). While both **1a** and **1b** are the minima on the potential surface, **1a** is 9.0 kcal/mol more stable than **1b**. Because of the unfavorability of two *trans* hydrides in **1b**, the Ir–H bond lengths in **1b** are 0.08 Å longer than those in **1a**, and the Ir–C(^{H}PCP) bond length is 0.09 Å shorter than that in **1a**. The TS between **1a** and **1b** is only 0.4 kcal/mol higher in energy than **1b** and shows a surprisingly unsymmetrical structure in which one of the C^{PCP}–Ir–H is 79.9°

Scheme 2.

Fig. 1. The calculated energies for the intermediates involved in the transfer reaction by Li and Hall [59].

and the other is 112.5°. This result has been attributed an orbital crossing between occupied and empty orbitals in the symmetric transformation from **1a** to **1b** [85]. The pathway involving **1a** is named the exopathway because the alkane approaches the metal from the "side" (at the larger C–Ir–H angle), and the pathway involving **1b** is named the endopathway because the alkane approaches the metal from the "front" (at the larger H–Ir–H angle). Except for the 9.0 kcal/mol energy difference between **1a** and **1b**, intermediates and TSs are similar for these two pathways. Since the exopathway is lower in energy, we will focus on this pathway in both the transfer and the acceptorless reactions in the alkane dehydrogenation reaction. The differences between exo- and endopathways will be addressed briefly in the discussion.

3.1. Transfer dehydrogenation reaction

The transfer reaction's mechanism is quite different because it first utilizes a sacrificial alkene to remove the dihydrogen from the pincer complex. In their study, Li and Hall used ethylene as the hydrogen acceptor and ethane as the reactant to survey the potential energy surface of this reaction [59]. Their study revealed
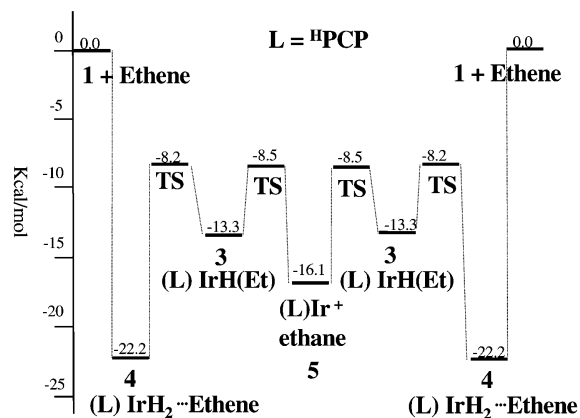
that the sacrificial ethylene also can attack the metal center in two directions relative to the H–Ir–H angle. Again, only the exopathway is diagrammed in Fig. 1. A 'prime' is used to distinguish between the intermediates and TSs with the sacrificial alkene (CH_2CHR') and the ones with the target alkane (CH_3CH_2R). Of course, the model used $R'=R=H$.

3.2. Elimination of dihydrogen with transfer mechanism

In the first step of the transfer reaction, ethylene was found to bind strongly to the (^HPCP)Ir(H)$_2$ complex; the average Ir–C(ethylene) bond lengths are 2.25 Å for **4'** and it is 22.2 kcal/mol more stable than **1** + ethylene. In the next step, the reverse of β-H transfer, one of the hydrides transfers onto ethylene to make the (^HPCP)Ir(H)(ethyl) complex, **3'**. This step has a barrier of 14.0 kcal/mol and **3'**, an ethyl complex, is 10.6 kcal/mol less stable than **4'**, the ethene complex. There is no oxidation-state change in this step of the reaction. In order to complete the elimination of the dihydrogen, the second hydride and the alkyl (ethyl) must be reductively eliminated to make an agostic ethane complex. Despite the oxidation state change from Ir(III) to Ir(I), this step has a lower barrier (4.8 kcal/mol) than the first hydride transfer and **5**, the agostically bound ethane complex, is more stable than **3'** by 2.8 kcal/mol. The product of this elimination step is the 14-electron (^HPCP)Ir(I).

3.3. Oxidative addition of alkane with transfer reaction

As pointed out early, the second phase of the transfer reactions is the reverse of the steps described above. Thus, the next step, oxidative addition of the target alkane (in this case, ethane) is simply the reverse of step from **3′** to **5** in Section 3.2. Although the target alkane (CH_3CH_2R) in the experimental systems are different from the sacrificial one (CH_3CH_2R'), the previous theoretical study [58] calculated the energy profile with $R=R'=H$. Therefore, the oxidative addition of ethane to (^HPCP)Ir(I), **5**, overcomes a barrier of 7.6 kcal/mol and is endoergic by 2.8 kcal/mol in forming the intermediate, (^HPCP)Ir(III)(H)(ethyl) species **3**. The energy barriers required for the transfer reaction is slightly smaller than those for the acceptorless reaction (see following sections).

3.4. Oxidative addition of the alkane with acceptorless associative reaction

Species **3** (earlier) is a key intermediate in both the transfer and the acceptorless reaction, but it is reached by a quite different route in the acceptorless reaction as this reaction requires no sacrificial hydrogen acceptor and produces H_2 as a byproduct. Initial calculations suggested that the direct acceptorless reduction elimination of H_2 (from **1** to **5**) was high in energy and that the high barrier would prevent this dissociation reaction from becoming important [58]. However, at high enough temperature, entropy will cause this reaction to become favorable (vida infra).

The first step in the lowest energy mechanism is the oxidative addition of alkane, which proceeds through a TS with barrier of 19.0 kcal/mol for the exopathway and produces intermediate **2** which is an Ir(V) alkyl trihydride species. Intermediate **2** shows a pentagonal bipyramidal structure and is 10.9 kcal/mol less stable than **1** + alkane.

3.5. Reductive elimination of dihydrogen with acceptorless reaction

The next step for the low-energy acceptorless mechanism involves elimination of dihydrogen from the trihydride intermediate **2**. Two different pairs of H_2
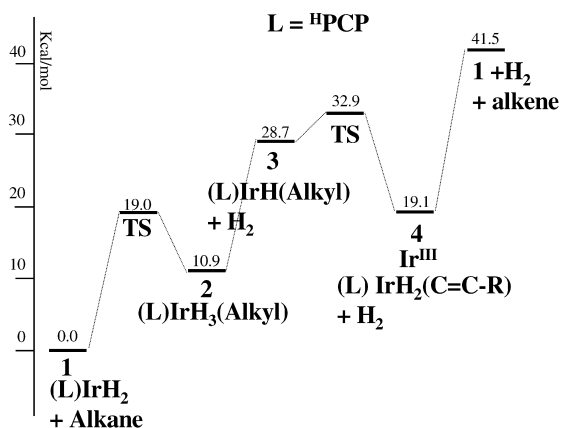

Fig. 2. The calculated energies for the intermediates involved in the acceptorless reaction by Niu and Hall [58], which are in a somewhat smaller basis in Fig. 1.

could be eliminated from **2**. Only one of these pairs is predicted to lead to a "stable" dihydrogen complex before its elimination. The stable complex forms when the dihydrogen is *trans* to the carbon atom of the pincer ligand, while no H_2 complex exists when the dihydrogen is reductively eliminated. Nevertheless, the potential surface is relative flat from trihydride complexes to dihydrogen complexes ($\sim$1.4 kcal/mol). The energy barrier required to eliminate the dihydrogen from the trihydride intermediate **2** (Ir(V) species) is 17.8 kcal/mol for an exopathway, which leads to the Ir(III) intermediate **3** (Fig. 2). This step not only reduces the formal oxidation state of Ir from the state V to III, but also creates a vacant site for the transfer of β-H.

3.6. β-Hydrogen transfer and cleavage of coordinated olefin in both reactions

Since these two steps ($3 \rightarrow 4 \rightarrow 1$) are essentially the same for both reactions, we will discuss them together. Because the basis set used for ^HPCP ligand by Li and Hall [59] is larger than that used in the earlier calculations by Niu and Hall [58], the calculated barriers and intermediates are slightly different. As an example of the dependence on basis set, we will present Niu and Hall's results in parenthesis for the exopathway in the following discussion. Again only the exopathway is presented in Figs. 1 and 2.

Intermediate **3** has an agostic C–H bond from the alkyl ligand and may undergo rearrangement to produce a β-H agostic intermediate. However, it must be in an eclipsed conformation for C_α–C_β before transfer of the β-H to the metal. These rearrangements are typically in the range of 2–4 kcal/mol. When the β-H is in close (agostic) contact with the metal and the α, β carbons are in the eclipse conformation, the barriers for β-H transfer are 5.1 (4.2) kcal/mol for the exopathway. The product of this β-H transfer is the olefin-bound pincer dihydride complex **4** and **3** → **4** is 10.9 (9.6) kcal/mol exoergic.

The last step is the loss of the coordinated olefin. This step is endoergic by 22.2 (22.4) kcal/mol for the exopathway. The energy for the cleavage of olefin from the (^{H}PCP)IrH$_2$(olefin) is 18.4 kcal/mol less than that calculated for the CpIr(H)(PH$_3$)(olefin)$^+$ system [58]. This difference and closely related differences are the reasons that the PCP complexes are such good catalysts for this reaction.

3.7. Energy barriers and dehydrogenation efficiency

Comparison of Figs. 1 and 2 provides an overview of how transfer and acceptorless dehydrogenation reactions differ. The energies in both figures are for the exopathway and are relative to species **1** plus alkane or alkene (as appropriate), which is referenced as 0.0 kcal/mol. Fig. 1 has the energies of Li and Hall [59] while Fig. 2 has the energies of Niu and Hall [58], which are from calculations in a somewhat smaller basis.

The model for the transfer reaction has zero overall energy change because the sacrificial alkene corresponds exactly to the alkane. Because of the strong bond between the alkene and the (^{H}PCP)IrH$_2$ complex, the energies for all intermediates and TSs of this transfer reaction are below zero. In contrast, because the high endothermicity of the acceptorless reaction, Alkane → Alkene + H$_2$, the energies for its intermediates and TSs appear quite high in energy. Therefore, the best way to compare these two reactions, which have such different overall thermodynamics, is to compare their critical barriers.

The critical barriers for the transfer reaction are from **4′** to **3′** (first hydride transfer to a sacrificial

alkene in the elimination of dihydrogen), from **5** to **3** (oxidative addition of alkane) and **4** to **1** (loss of olefin), which are 14.0, 7.6, and 22.2 kcal/mol for exopathway. The endopathway barriers in the transfer reaction (14.9, 11.6 and 27.8 kcal/mol) are not as well-balanced as those for the exopathway. In particular, the last barrier is much higher because the stronger bonding in **1b** between the coordinated olefin and the metal makes this olefin-loss step more difficult.

From Fig. 2, one can see that the critical steps for the acceptorless dehydrogenation reaction are from **1** to **2** (oxidative addition of alkane), from **2** to **3** (reductive elimination of dihydrogen), and from **4** to **1** (loss of olefin), which have barriers of 19.0, 17.8, and 22.4 kcal/mol, respectively. The related Ir(III) complex CpIr(H)(PR$_3$)$^+$, which has not been shown to catalyze this reaction, has higher critical barriers for reductive elimination of dihydrogen (24.3 kcal/mol) and loss of olefin (40.8 kcal/mol) [58]. The more evenly distributed barriers for the pincer reaction, where no TS is higher than the overall endothermicity and no intermediate is more stable than the reactant, may contribute to its efficiency in catalyzing the dehydrogenation [58]. Besides an initial barrier of 9.4 kcal/mol between **1a** and **1b**, the endopathway has three critical barriers at 15.8, 12.7, 32.8 kcal/mol, respectively; again the third barrier much higher than the other two.

Krogh-Jespersen et al. studied the entropy contribution to these reactions starting with (^{Me}PCP)Ir(III)H$_2$ and (^{Me}PCP)Ir(I) complexes [65]. By extrapolating these gas-phase free energy calculations to higher temperature condensed-phase chemistry, they suggest that even with higher barriers the acceptorless reaction would proceed by a dissociative pathway (Scheme 2) through intermediate **5**. In our most recent work [57], we surveyed alternative reaction pathways using a slight different catalyst, (anthraphos)Ir(III)H$_2$: the acceptorless dissociative pathway where dihydrogen is lost before oxidative addition of alkane [25,65], an acceptorless interchange pathway where the loss of dihydrogen and oxidative addition of alkane are in concert, and the associative pathway [58,65] discussed in detail earlier (see Scheme 2). Our results on this system suggest that at the elevated temperature employed for the reaction (523 K), the dissociative, interchange and acceptorless pathways are all accessible by the pincer-like complex.

4. Conclusions

Alkane dehydrogenation by the transfer reaction and the acceptorless reaction may access different reaction pathways and intermediates. However, both reactions show three critical reaction barriers: oxidative addition of alkane, reductive elimination, and loss of olefin and both have a key intermediate: species **3**. This key intermediate **3** is a 16-electron (PCP)Ir(III)(H)(alkyl) complex and both reactions will go through this species before go through β-H transfer, **3 → 4**, and loss of olefin, **4 → 1**, as shown in Scheme 2. These two reactions follow different reaction steps to get to species **3**. For example, the transfer reaction can utilize a hydrogen acceptor to produce a 14-electron intermediate of (PCP)Ir(I), **5**, before it forms species **3**, while the acceptorless reaction can produce an 18-electron intermediate of (PCP)Ir(V)(H)$_3$(Alkyl), **2**, before it reaches intermediate **3**.

These three critical reaction barriers are balanced in both the transfer reaction and the acceptorless reaction. However, the related CpIr(H)(PR$_3$)$^+$ complex, which could undergo similar reaction steps, has unbalanced reaction barriers, where one of the intermediate is more stable than the reactant. This difference can be attributed to a much more rigid *mer* geometric structure of the pincer complex, which results in a less favorable olefin–metal interaction and increases the energy difference between the singlet and triplet states of this pincer complex. Therefore, both the particular geometric arrangement and the well-balanced critical barriers make the pincer complex an efficient catalyst for alkane dehydrogenation.

Although calculations on the pincer complexes have shown that the associative mechanism is the lower energy one between the two pathways at the room temperature, the similar anthraphos iridium complex suggests that, in addition to the associative mechanism, the dissociative and interchange pathways may be accessible at the elevated temperature with the consideration of the entropy contribution. In another words, the oxidation states of iridium from Ir(I) to Ir(V) could be accessible by all reaction pathways at a high reaction temperature. Therefore, the stability of these homogenous catalysts at high temperature will be as equally important as the geometric arrangement of catalysts and the barrier distributions for the alkane dehydrogenation.

References

[1] C.G. Jia, T. Kitamura, Y. Fujiwara, Acc. Chem. Res. 34 (2001) 633–639.
[2] C. Slugovc, I. Padilla-Martinez, S. Sirol, E. Carmona, Coord. Chem. Rev. 213 (2001) 129–157.
[3] F. Kakiuchi, S. Murai, in: S. Murai (Ed.), Activation of Unreactive Bonds and Organic Synthesis, Springer, Berlin, 1999, p. 47.
[4] A.E. Shilov, G.B. Shul'pin, Chem. Rev. 97 (1997) 2879–2932.
[5] B.A. Arndtsen, R.G. Bergman, T.A. Mobley, T.H. Peterson, Acc. Chem. Res. 28 (1995) 154–162.
[6] C.L. Hall, Activation and Functionalization of Alkanes, Wiley, New York, 1989.
[7] R.H. Crabtree, Chem. Rev. 85 (1985) 245–269.
[8] M.J. Burk, R.H. Crabtree, C.P. Parnell, R.J. Uriarte, Organometallics 3 (1984) 816–817.
[9] M.J. Burk, R.H. Crabtree, D.V. McGrath, Chem. Commun. (1985) 1829–1830.
[10] M.J. Burk, R.H. Crabtree, J. Am. Chem. Soc. 109 (1987) 8025–8032.
[11] K. Nomura, Y. Saito, Chem. Commun. (1988) 161–162.
[12] K. Nomura, Y. Saito, J. Mol. Catal. 54 (1989) 57–64.
[13] T. Sakakura, T. Sodeyama, M. Tanaka, New J. Chem. 13 (1989) 737–745.
[14] J.A. Maguire, W.T. Boese, A.S. Goldman, J. Am. Chem. Soc. 111 (1989) 7088–7093.
[15] T. Sakakura, F. Abe, M. Tanaka, Chem. Lett. (1991) 297–298.
[16] M. Gupta, C. Hagen, R.J. Flesher, W.C. Kaska, C.M. Jensen, Chem. Commun. (1996) 2083–2084.
[17] M. Gupta, C. Hagen, W.C. Kaska, R.E. Cramer, C.M. Jensen, J. Am. Chem. Soc. 119 (1997) 840–841.
[18] M. Gupta, W.C. Kaska, C.M. Jensen, Chem. Commun. (1997) 461–462.
[19] R.H. Crabtree, J.M. Mihelcic, J.M. Quirk, J. Am. Chem. Soc. 101 (1979) 7738–7740.
[20] D. Baudry, M. Ephritikhine, H. Felkin, R. Holmes-Smith, Chem. Commun. (1983) 788–789.
[21] J.A. Maguire, A.S. Goldman, J. Am. Chem. Soc. 113 (1991) 6706–6708.
[22] T. Fujii, Y. Higashino, Y. Satio, J. Chem. Soc., Dalton Trans. (1993) 517–520.
[23] J. Belli, C.M. Jensen, Organometallics 15 (1996) 1532–1534.

[24] D.W. Lee, W.C. Kaska, C.M. Jensen, Organometallics 17 (1998) 1–3.
[25] C.M. Jensen Chem. Commun. (1999) 2443–2449.
[26] W.W. Xu, G.P. Rosini, M. Gupta, C.M. Jensen, W.C. Kaska, K. Krogh-Jespersen, A.S. Goldman, Chem. Commun. (1997) 2273–2274.
[27] F. Liu, A.S. Goldman, Chem. Commun. (1999) 655–656.
[28] H. Takaya, S.I. Murahashi, Synlett. (2001) 991–994.
[29] S. Busch, L. Leitner, Adv. Synth. Catal. 343 (2001) 192–195.
[30] D.G. Gusev, F.M. Dolgushin, M.Y. Antipin, Organometallics 20 (2001) 1001–1007.
[31] R.M. Gauvin, H. Rozenberg, L.J.W. Shimon, D. Milstein, Organometallics 20 (2001) 1719–1724.
[32] P. Barrio, R. Castarlenas, M.A. Esteruelas, E. Onate, Organometallics 20 (2001) 2635–2638.
[33] T.B. Wen, Y.K. Cheung, J.Z. Yao, W.T. Wong, Z.Y. Zhou, G.C. Jia, Organometallics 19 (2000) 3803–3809.
[34] A. Sundermann, O. Uzan, J.M.L. Martin, Organometallics 20 (2001) 1783–1791.
[35] V.V. Grushin, W.J. Marshall, D.L. Thorn, Adv. Synth. Catal. 343 (2001) 161–165.
[36] D.H. Woodmansee, X.H. Bu, G.C. Bazan, Chem. Commun. (2001) 619–620.
[37] H.M.L. Davies, E.G. Antoulinakis, J. Organomet. Chem. 617 (2001) 47–55.
[38] J.T. Golden, R.A. Andersen, R.G. Bergman, J. Am. Chem. Soc. 123 (2001) 5837–5838.
[39] T.H. Peterson, J.T. Golden, R.G. Bergman, J. Am. Chem. Soc. 123 (2001) 455–462.
[40] P.J. Alaimo, B.A. Arndtsen, R.G. Bergman, Organometallics 19 (2000) 2130–2143.
[41] K. Tani, T. Yamagata, Y. Kataoka, K. Mashima, J. Synth. Org. Chem. Jpn. 57 (1999) 656–666.
[42] E.A. Grigoryan, Kinet. Catal. 40 (1999) 350–363.
[43] B. Martin-Matute, C. Mateo, D.J. Cardenas, A.M. Echavarren, Chem. Eur. J. 7 (2001) 2341–2348.
[44] M. Catellani, F. Cugini, D. Tiefenthaler, Can. J. Chem. 79 (2001) 742–751.
[45] X.G. Fang, B.L. Scott, J.G. Watkin, G.J. Kubas, Organometallics 19 (2000) 4193–4195.
[46] M. Catellani, E. Motti, S. Ghelli, Chem. Commun. (2000) 2003–2004.
[47] M.A. Zhuravel, N.S. Grewal, D.S. Glueck, K.C. Lam, A.L. Rheingold, Organometallics 19 (2000) 2882–2890.
[48] L. Johansson, O.B. Ryan, C. Romming, M. Tilset, J. Am. Chem. Soc. 123 (2001) 6579–6590.
[49] U. Fekl, W. Kaminsky, K.I. Goldberg, J. Am. Chem. Soc. 123 (2001) 6423–6424.
[50] S. Reinartz, P.S. White, M. Brookhart, J.L. Templeton, J. Am. Chem. Soc. 123 (2001) 6425–6426.
[51] J.C. Thomas, J.C. Peters, J. Am. Chem. Soc. 123 (2001) 5100–5101.
[52] S. Reinartz, P.S. White, M. Brookhart, J.L. Templeton, Organometallics 20 (2001) 1709–1712.
[53] L.R. Falvello, S. Fernandez, C. Larraz, R. Llusar, R. Navarro, E.P. Urriolabeitia, Organometallics 20 (2001) 1424–1436.
[54] C.J. Moulton, B.L. Shaw, J. Chem. Soc., Dalton Trans. (1976) 1020–1024.
[55] M. Gandelman, A. Vigalok, L.J.W. Shimon, D. Milstein, Organometallics 16 (1997) 3981–3986.
[56] M. Gerisch, J.R. Krumper, R.G. Bergman, T.D. Tilley, J. Am. Chem. Soc. 123 (2001) 5818–5819.
[57] M.W. Haenel, S. Oevers, K. Angermund, W.C. Kaska, H.J. Fan, M.B. Hall, Angew. Chem. Int. Ed. 40 (2001) 3596–4000.
[58] S. Niu, M.B. Hall, J. Am. Chem. Soc. 121 (1999) 3992–3999.
[59] S. Li, M.B. Hall, Organometallics 20 (2001) 2153, errata: 20 (2001) 3210.
[60] D. Strout, S. Zaric, S. Niu, M.B. Hall, J. Am. Chem. Soc. 118 (1996) 6068–6069.
[61] M.D. Su, S.Y. Chu, J. Am. Chem. Soc. 119 (1997) 5373–5383.
[62] Y.Z. Han, L.Q. Deng, T. Ziegler, J. Am. Chem. Soc. 119 (1997) 5939–5945.
[63] S. Niu, M.B. Hall, J. Am. Chem. Soc. 120 (1998) 6169–6170.
[64] R. Jimenez-Catano, S. Niu, M.B. Hall, Organometallics 16 (1997) 1962–1968.
[65] K. Krogh-Jespersen, M. Czerw, M. Kanzelberger, A.S. Goldman, J. Chem. Inform. Comput. Sci. 41 (2001) 56–63.
[66] R.G. Parr, W. Yang, Density–Functional Theory of Atoms and Molecules, Oxford University Press, New York, 1989.
[67] A.D. Becke, Phys. Rev. A38 (1988) 3098–3100.
[68] A.D. Becke, J. Chem. Phys. 98 (1993) 1372–1377.
[69] A.D. Becke, J. Chem. Phys. 98 (1993) 5648–5652.
[70] C. Lee, W. Yang, R.G. Parr, Phys. Rev. B37 (1988) 785–789.
[71] H.B. Schlegel, Theor. Chim. Acta 66 (1984) 333–340.
[72] J.B. Foresman, A.E. Frish, Exploring Chemistry with Electronic Structure Methods, Gaussian, Inc., Pittsburgh, PA, 1993
[73] LANL2DZ: Dunning D95 basis sets on first row, Los Alamos ECP plus double-zeta basis set on Na–Bi.
[74] P.J. Hay, W.R. Wadt, J. Chem. Phys. 82 (1985) 299–310.
[75] M. Couty, M.B. Hall, J. Comput. Chem. 17 (1996) 1359–1370.
[76] A. Hollwarth, M. Bohme, S. Dapprich, A.W. Ehlers, A. Gobbi, V. Jonas, K.F. Kohler, R. Stegmann, A. Veldkamp, G. Frenking, Chem. Phys. Lett. 208 (1993) 237–240.
[77] T.H. Dunning Jr., P.J. Hay, in: H.F. Schaefer III (Ed.), Modern Theoretical Chemistry, Vol. 3, Plenum Press, New York, 1976.
[78] P.C. Harihara, J.A. Pople, Theor. Chim. Acta 28 (1973) 213–222.
[79] W.J. Hehre, L. Radom, P.V.R. Schleyer, J.A. Pople, Ab initio Molecular Orbital Theory, Wiley, New York, 1986.
[80] A.D. McLean, G.S. Chandler, J. Chem. Phys. 72 (1980) 5639–5648.
[81] R. Krishnan, J.S. Binkley, R. Seeger, J.A. Pople, J. Chem. Phys. 72 (1980) 650–654.
[82] J.S. Binkley, J.A. Pople, W.J. Hehre, J. Am. Chem. Soc. 102 (1980) 939–947.
[83] M.E. Van der Boom, C.L. Higgitt, D. Milstein, Organometallics 18 (1999) 2413–2419.
[84] B.A. Arndtsen, R.G. Bergman, Science 270 (1995) 1970–1973.
[85] J.F. Riehl, Y. Jean, O. Eisenstein, M. Pelissier, Organometallics 11 (1992) 729–737.